
MIX FROM FAILURE: CONFUSION-PAIRING MIXUP FOR LONG-TAILED RECOGNITION

Youngseok Yoon
UCSB
California, USA
youngseok_yoon@ucsb.edu

Sangwoo Hong
Seoul National University
South Korea
swhong@cml.snu.ac.kr

Hyungjun Joo
Seoul National University
South Korea
joojh911@cml.snu.ac.kr

Yao Qin
UCSB, Google
California, USA
yaoqin@ucsb.edu

Haewon Jeong
UCSB
California, USA
haewon@ucsb.edu

Jungwoo Lee
Seoul National University
South Korea
junglee@snu.ac.kr

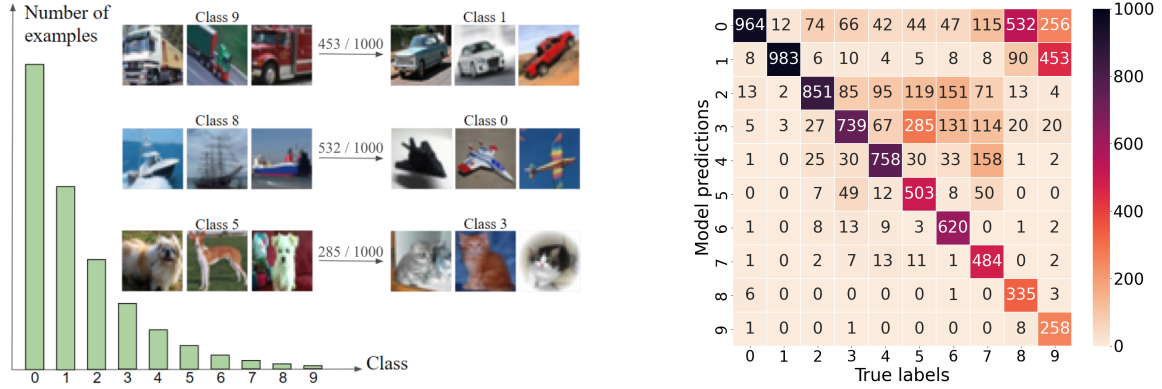
ABSTRACT

Long-tailed image recognition is a computer vision problem considering a real-world class distribution rather than an artificial uniform. Existing methods typically detour the problem by i) adjusting a loss function, ii) decoupling classifier learning, or iii) proposing a new multi-head architecture called experts. In this paper, we tackle the problem from a different perspective to augment a training dataset to enhance the sample diversity of minority classes. Specifically, our method, namely Confusion-Pairing Mixup (CP-Mix), estimates the confusion distribution of the model and handles the data deficiency problem by augmenting samples from confusion pairs in real-time. In this way, CP-Mix trains the model to mitigate its weakness and distinguish a pair of classes it frequently misclassifies. In addition, CP-Mix utilizes a novel mixup formulation to handle the bias in decision boundaries that originated from the imbalanced dataset. Extensive experiments demonstrate that CP-Mix outperforms existing methods for long-tailed image recognition and successfully relieves the confusion of the classifier.

1 Introduction

Large-scale datasets [1, 2], algorithmic innovations [3, 4], and powerful network architectures [5, 6] have driven remarkable achievements in computer vision over recent decades. However, these advancements primarily rely on clean, well-curated datasets like CIFAR-100 or ImageNet, which are balanced with a comparable amount of samples for each image class. In contrast, real-world data collection processes often result in biased and imbalanced datasets with a long-tail distribution. This distribution is characterized by a large number of minority classes containing very few samples, while the majority of samples belong to a small number of majority classes. Consequently, the standard training strategy based on empirical risk minimization struggles to generalize effectively to minority classes, leading to poor performance in these categories.

Given the prevalence of long-tailed data in practical scenarios, numerous research efforts have been directed toward addressing long-tailed problems. An intuitive approach to addressing this issue is data augmentation, as the key challenge is the lack of samples in minority classes. However, implementing data augmentation is not straightforward in such contexts due to the extreme scarcity of minority samples. Often, the majority classes benefit more from the augmentation method, further enlarging the discrepancy between majority and minority classes. To address these challenges, researchers have explored simpler methods by synthesizing minority data points, using techniques such as SMOTE and its variations [7, 8, 9]. One such approach is ‘*Mixup*’, which linearly interpolates two existing data points to create a new data point [10]. Despite its conceptual simplicity, Mixup has proven effective in improving generalization [11, 12, 13, 14, 15, 16, 17, 18] and long-tailed learning [19, 20, 21, 22, 23, 24].



(a) Class distribution of an imbalanced training set CIFAR10-LT-200 and (b) Confusion matrix of the classifier trained using the model's misclassification tendency.

Figure 1: (a) The model's tendency to misclassify the examples in the minorities (truck, ship, and dog) to their similar majorities (car, plane, and cat). **The model captures the similarities between classes and wrongly exploits its capacity.** (b) The confusion matrix of the model trained using the imbalanced dataset. x and y axis denote true labels and predictions, respectively, and each number in a cell denotes the number of predictions. **There are clear relationships between semantically similar classes.**

In this paper, we focus on effectively applying Mixup in scenarios with a large number of severely imbalanced classes. We first demonstrate that Mixup does not improve prediction accuracy for minority groups when extreme imbalances exist in the data distribution. Instead, it amplifies the performance gap between majority and minority groups because Mixup does not consider class imbalance or relationships among different classes. Vanilla Mixup randomly samples two data points from the training set, which becomes increasingly ineffective for imbalanced and complex datasets due to the difficulty of sampling minority classes and pairing them with confusing classes. To address this, we developed the confusion-pairing mixup (CP-Mix) method, which specifically samples from 'confusion pairs' that are prone to misclassification. With this modification, we significantly improve minority accuracy, even when the imbalance factor is as high as 996, e.g., for Places-LT. In vanilla Mixup, samples from minority groups are rarely used and often paired with unrelated classes. Our method focuses on minority classes, pairing them with useful samples to enhance model generalization. Through an ablation study, we demonstrate that strategic sampling from confusion pairs is the primary contributor to our method's improved performance.

While many strategies address the long-tailed problem, we believe that our proposed CP-Mix is uniquely strong as a simple yet powerful tool. First, it provides better generalization than approaches based on re-weighting or re-sampling [25, 26, 27, 28, 29, 30] or modifying the objective function [31, 32, 33, 34, 35, 36], which often lead to overfitting and memorization of minority samples. Secondly, CP-Mix requires significantly less computation than solutions based on training multiple-experts [37, 38, 39, 40, 41, 42]. Finally, it is easy to implement on top of any existing learning algorithm, being model-agnostic.

To summarize our contributions:

- We identify a novel problem that vanilla mixup strategies exhibit a bias-amplifying phenomenon under very-long-tailed regimes where we have a large number of classes and the imbalance is significant between majority and minority classes.
- We propose CP-Mix algorithm that combines ideas of confusion pair sampling and class-imbalance-aware mixing to achieve more targeted intervention on the most vulnerable pairs while achieving generalization.
- We provide through experimental evaluation that CP-Mix achieves improvements over baselines in various long-tailed datasets.

This paper is organized as follows. Section 2 introduces the background of long-tailed recognition and mixup augmentation. Then, we discuss how imbalance in the training set affects the models and how mixup cannot improve them in Section 3. CP-Mix is described in Section 4, and its superiority is demonstrated in Section 5 through extensive experiments.

2 Background and Related Works

2.1 Long-tailed image classification

Long-tailed recognition aims to train a model that performs well given a training dataset with a long-tailed distribution. We target an image classification task that the class distribution is severely imbalanced with C classes. Let the training dataset $\mathcal{D}_s = \{(x_i, y_i)\}_{i=0}^{N-1}$ consists of N training points where x_i and y_i denote an input and its corresponding class label, sampled from the input space \mathcal{X} and the label set $\mathcal{C} = \{0, \dots, C-1\}$, respectively. \mathcal{D}_s is an union of C disjoint subsets \mathcal{D}_c for $c \in \mathcal{C}$ where $\mathcal{D}_c = \{(x_i, y_i) | (x_i, y_i) \in \mathcal{D}_s, y_i = c\}$. We denote the cardinality of a subset \mathcal{D}_c as n_c where $\sum_{c=0}^{C-1} n_c = N$ and $n_0 > n_1 > \dots > n_{C-1}$ without loss of generality. We also denote an imbalance factor of \mathcal{D}_s as $\rho = n_0/n_{C-1} \gg 1$.

We term $f_\theta : \mathcal{X} \rightarrow \mathbb{R}^C$ as a model parameterized by learnable parameters θ that maps an input to a label and a prediction as $\hat{y}_\theta(x) = \arg \max f_\theta(x)$. With a bit of abuse of notations, we use y to denote both the class label and its one-hot vector. The ERM objective is denoted by

$$\mathcal{L}_{ERM}(\theta, l) = \mathbb{E}_{(x,y) \sim \mathcal{P}}[l(f_\theta(x), y)] \approx \frac{1}{N} \sum_{(x_i, y_i) \in \mathcal{D}_s} l(f_\theta(x_i), y_i), \quad (1)$$

where \mathcal{P} and $l(f_\theta(x), y)$ are the data distribution and sample-wise classification loss, respectively.

2.2 Mixup

Mixup [10] is a simple and effective data augmentation strategy that linearly interpolates samples (x_1, y_1) and (x_2, y_2) to improve the generalization capacity of the model. Using a linear interpolation function $M(d_1, d_2, \lambda) = \lambda \times d_1 + (1 - \lambda) \times d_2$ for internal division where d is input or label and $\lambda \in [0, 1]$, mixup formulation can be written as

$$\tilde{x}_{mix} = \lambda \times x_1 + (1 - \lambda) \times x_2 = M(x_1, x_2, \lambda), \quad (2)$$

$$\tilde{y}_{mix} = \lambda \times y_1 + (1 - \lambda) \times y_2 = M(y_1, y_2, \lambda), \quad (3)$$

where y_1 and y_2 are one-hot vectors of labels, and λ is sampled from a random distribution. Based on theoretical analysis and symmetry of data distribution, the authors of [10] proposed to use Beta distribution to sample $\lambda \sim \text{Beta}(\alpha, \alpha)$. To avoid confusion, we denote λ and α as a mixing parameter and mixup hyperparameter, respectively.

Mixup uses $(\tilde{x}_{mix}, \tilde{y}_{mix})$ instead of real data points to train the model. The learning objective is

$$\mathcal{L}_{Mixup}(\theta, l) = \mathbb{E}_{(\tilde{x}, \tilde{y}) \sim \tilde{\mathcal{P}}} [l(f_\theta(\tilde{x}), \tilde{y})] \approx \frac{1}{N'} \sum_{(\tilde{x}_i, \tilde{y}_i) \in \tilde{\mathcal{D}}_s} l(f_\theta(\tilde{x}_i), \tilde{y}_i), \quad (4)$$

where $\tilde{\mathcal{P}}$ and $\tilde{\mathcal{D}}_s$ are the distribution and dataset with cardinality N' of mixed samples $(\tilde{x}_{mix}, \tilde{y}_{mix})$.

With negligible additional computation, mixup converts the empirical risk minimization (ERM) into the vicinal risk minimization (VRM) [43]. Inspired by its simplicity, many extensions have been proposed to interpolate samples in manifold space [11], randomly crop a patch in an image and replace it with another patch from another image [12], utilize self-augmentation to generate new samples [13] and use a saliency map to augment contextual information [14, 15, 17]. Also, theoretical aspects of mixup are considered in many works [44, 45, 46, 47].

Recently, RegMixup [48] has been proposed to use a mixup objective as a regularization for VRM instead of a sole training objective. Based on a thorough analysis, RegMixup argues that combining ERM and mixup objectives improves generalization and out-of-distribution robustness simultaneously. In this paper, we combine the mixup objective revised for the long-tailed training set with the ERM objective.

2.2.1 Mixup for long-tailed image recognition

Several works have tried to handle long-tailed image classification using Mixup. Remix [19] considers the imbalance ratio to determine the mixed labels. The iterative algorithm is used in Mixboost [20] to synthesize additional samples in imbalanced datasets. The authors of [49] use mixup as a trick to boost long-tailed visual recognition. Also, authors of [46, 21] solve the problem of mis-calibrated model using mixup in the long-tailed distribution. CMO [22] uses the Cutmix [12] to synthesize new samples from the background of majorities and instances of minorities. CSA [23] effectively augments the training samples by removing irrelevant contexts. The most related work to ours is OTMix [24] which learns the relationships between classes and utilizes CutMix for augmentation. Unlike previous works, we propose a novel approach to regularize the model by mixing samples from confusing classes estimated from the training set in real-time to compensate for the weak points.

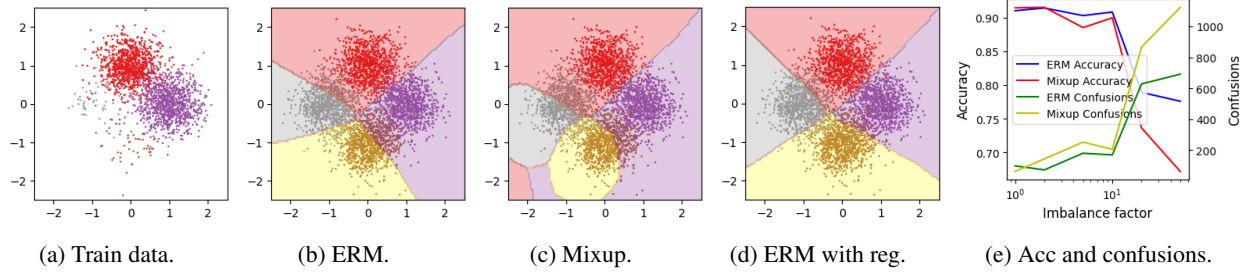


Figure 2: (a) 2D 4-way toy example with 1000 and 50 samples in majority and minority classes. The majority classes red and purple are similar to minorities grey and yellow, respectively. (b-d) Decision boundaries of the classifiers on a balanced test dataset. (b, c) **The ERM classifier has a biased boundary toward minorities, and the Mixup classifier has a more restricted region for minorities since Mixup mainly occurs between and within red and purple points.** (d) The ERM classifier regularized by a mixup objective where similar majority and minority classes are mixed. **Mixup occurs between red and grey points or purple and yellow points for the regularization. It successfully improves the decision boundary while maintaining the structure of the boundary.** (e) Accuracy and confusion of ERM classifier as imbalance factors vary. Confusion denotes the sum of confusion values between two pairs of adjacent majority and minority, grey points in red region and yellow points in purple region. **Although Mixup improves generalization in small imbalances, it fails as the imbalance factor increases.**

3 Confusion Tendency under Long-Tailed Distribution

When a classifier is trained on an imbalanced training set, it struggles to distinguish similar classes with different numbers of samples in the training set. It tends to classify minority samples as the majority counterpart, resulting in inferior performance. It is an important and serious problem as it commonly occurs in real-world datasets but is not observable in balanced training.

We define confusion of the model f_θ from class c_i to c_j on dataset \mathcal{D} as

$$C_{i,j}(f_\theta, \mathcal{D}) = |\{(x, c_i, c_j) | f_\theta(x) = c_j, (x, c_i) \in \mathcal{D}\}|, \quad (5)$$

to evaluate how much the model f_θ confuses class c_i as c_j . When the distribution of $C_{i,j}$ differs from the uniform as shown in Figure 1(b), we can say the model has high confusion. Although Mixup can augment minority samples with negligible additional complexity, it has limitations in reducing high confusion $C_{i,j}$ in long-tailed distribution. In fact, Mixup focuses on the generalization of majorities for imbalanced training datasets, aggravating minority generalization. In this section, we investigate how mixup fails to resolve confusion and improve classification. Also, we conduct further analysis on confusion matrices to achieve a deeper understanding of long-tailed distribution¹.

3.1 Toy Example

This subsection describes how the decision boundary of the classifier trained on the imbalanced set is biased using a 4-way classification dataset on a 2D plane, as shown in Figure 2(a). The classifier trained using the ERM objective has a biased decision boundary, as shown in Figure 2(b), failing to achieve generalization in minorities. When we train a Mixup classifier on the same dataset, Mixup frequently occurs between and within red and purple majorities, providing negligible changes to the decision boundary between them. Instead, rare mixups containing minority samples make it harder for the classifier to learn the boundary surrounding minorities due to the randomness. Figure 2(c) demonstrates how mixup destroys the structure of the decision boundary related to minorities when data imbalance is not considered.

In Figure 2(e), we can observe the relationship between accuracy of ERM classifier and confusion $C_{i,j}$ as the imbalance factor ρ differs in the toy example. Confusions on the right axis denote the sum of misclassifications from minority classes to their adjacent majorities, grey points in red region and yellow points in purple region. The increase of ρ results in higher confusion between adjacent majority and minority and decreased accuracy. Moreover, the negative effect of mixup grows as there is a severe imbalance between majorities and minorities.

We regularized the ERM classifier using a mixup objective, where mixup occurs between similar majority and minority, to reduce the confusions. When the augmented samples between red and grey points, and purple and yellow points are used for regularization, the decision boundary is less biased, as shown in Figure 2(d). It demonstrates that mixup considering imbalance and similarity of classes are critical for improving the classifiers.

¹Confusions $C_{i,j}$ are non-diagonal values of confusion matrix.

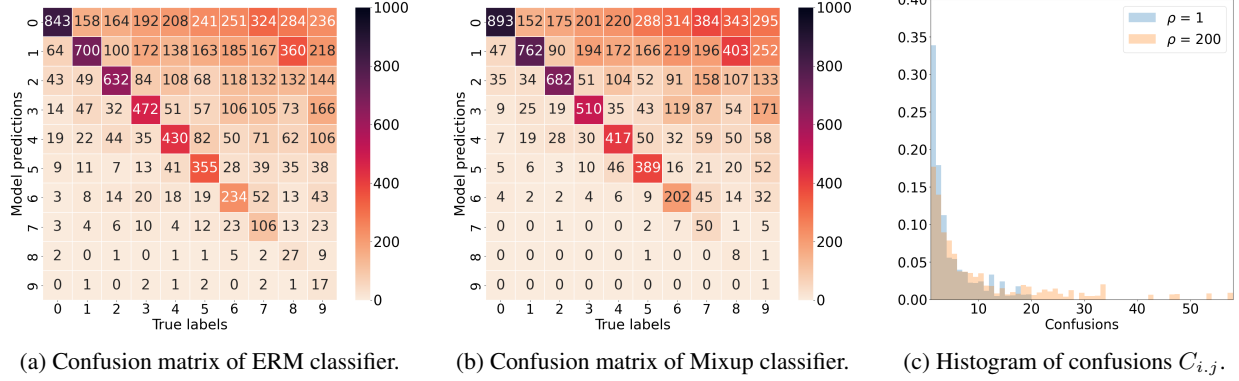


Figure 3: (a, b) Confusion matrices of ERM and Mixup classifiers trained on CIFAR100-LT dataset, respectively. The imbalance factor is 200, and classes are grouped into 10 subgroups for better visualization. **Mixup exacerbates the confusion of model, and only improves the generalization of majorities.** (c) Histogram of confusion values between pairs of classes for balanced CIFAR100 and CIFAR100-LT-200 datasets. Among 100 samples in each class, the maximum confusion value between two classes increases from 20 to more than 50 as ρ increases to 200.

3.2 CIFAR-LT

Similar problems are observed in classifiers trained in complex imbalanced datasets like CIFAR100-LT, as shown in Figure 3. We consolidate the 100 classes into 10 new groups, combining 10 classes into each group to simplify visualization. ERM classifier suffers from severe confusion, as demonstrated in the upper right region of confusion matrix in Figure 3(a). Most samples from minority classes are misclassified as majorities, while less than a hundred of ten thousand samples are predicted as the bottom 20 classes. Figure 3(b) demonstrates that sparsity of the bottom rows becomes more severe with Mixup, where less than a hundred samples are classified as bottom 30 classes. It shows that Mixup improves the generalization of majority groups rather than minorities, aggravating the bias of the classifiers.

We also observe a similar tendency of uneven confusion values $C_{i,j}$ for the ERM classifiers trained on CIFAR100-LT datasets. Figure 3(c) demonstrates the difference in confusion values between balanced and imbalanced datasets. While the maximum confusion value is less than 20 for the balanced CIFAR100 dataset, it increases to more than 50 out of 100 samples in a class as the imbalance factor becomes 200. Since the distribution of confusion values is long-tailed, more focus on the tail of confusion distribution is required for better performance. As we consider larger datasets with vast numbers of classes, it becomes more critical to concentrate specific pairs of classes in the tail distribution for Mixup since each pair is less likely to be sampled pairwise in random sampling.

4 Confusion-Pairing Mixup

We propose Confusion-Pairing Mixup (CP-Mix), which guides the model to classify confusing classes to improve minority generalization using mixup. Minority samples tend to be misclassified into some specific majority classes depending on the context and relation of classes when the train distribution is imbalanced, as shown in Figure 1. To handle this tendency, we propose estimating the model’s confusion distribution using the predictions from the imbalanced training set in real-time. Based on this estimation, CP-Mix samples and mixes data points, considering imbalances and confusions between classes. In the following subsections, the components of CP-Mix are described in detail.

4.1 Confusion-Pairs

CP-Mix estimates confusion distribution by collecting pairs of classes (c_t, c_m) that the model f_θ misclassifies an example x with a true label c_t as c_m . We use the imbalanced training set as a source to collect confusion pairs, so they are collected during the training phase. We denote a multiset (or bag) of these pairs as confusion-pairs \mathcal{CP}_e obtained from the current model at epoch e as:

$$\mathcal{CP}_e(\mathcal{D}_s) = [(c_t, c_m) | (x, c_t) \in \mathcal{D}_s, c_m = \hat{y}_\theta(x), c_t \neq c_m] \quad (6)$$

where the size of \mathcal{CP}_e is the number of misclassification at epoch e . We use square brackets to demonstrate a multiset to avoid confusion with a set. Multiset \mathcal{CP}_e allows the duplication of pairs so that it can describe the frequency of pairs². These confusion-pairs are accumulated to \mathcal{CP} so that the model can consider historical confusion tendencies. CP-Mix samples pairs from \mathcal{CP} and then data points given these pairs, while other mixup methods randomly match points in a mini-batch to synthesize new points. With CP-Mix, the model can concentrate more on class pairs of misclassifications and be trained to correct the confusion.

4.2 Mixing functions

Using different mixing parameters λ for input and label is a natural extension of vanilla mixup as below:

$$\tilde{x}_{mix} = \lambda_x \times x_1 + (1 - \lambda_x) \times x_2 = M(x_1, x_2, \lambda_x), \quad (7)$$

$$\tilde{y}_{mix} = \lambda_y \times y_1 + (1 - \lambda_y) \times y_2 = M(y_1, y_2, \lambda_y). \quad (8)$$

When the training dataset is severely imbalanced, the Mixup classifier learns a biased decision boundary, as shown in Figure 2(c) since it has been exposed to more samples mixed from samples in majority classes. To compensate for this behavior, mixed labels more favorable to minorities are required for a better decision boundary.

We propose to consider the imbalance of the training set for the label mixing function in Equation (8). Given a pair of examples (x_1, y_1) and (x_2, y_2) , our label mixing function considers the imbalance between two classes y_1 and y_2 as

$$\lambda_y(\lambda) = t \times \lambda + (1 - t) \times \frac{n_{y_2}}{n_{y_1} + n_{y_2}} \quad (9)$$

where t is a hyperparameter for label mixing and λ is sampled from beta distribution. With this formulation, the output of label mixing can be written as:

$$\tilde{y}_{CP} = M(y_1, y_2, \lambda_y(\lambda)) = M(M(y_1, y_2, \lambda), M(y_1, y_2, \frac{n_{y_2}}{n_{y_1} + n_{y_2}}), t). \quad (10)$$

This is equivalent to interpolating two terms: the first term can be thought of as a randomly mixed label, and the second term is mixed with a label-imbalance-aware parameter. While the first term provides generalization, as in vanilla Mixup, the second term tackles the underlying label imbalance in the training set. Our unique approach departs from the method employed in Remix [19], which uses an imbalance ratio for a threshold to decide the mixing parameter, and aims to achieve generalization alongside label imbalance mitigation. We use a randomly sampled λ for input mixing parameter, as in the vanilla Mixup.

4.3 CP-Mix

If \mathcal{CP} is used from the beginning of training, there exist two problems. First, minorities would be repeatedly used in the training, accelerating the overfitting on minorities. As a result, pairs including minorities would not be collected after a few epochs. Second, \mathcal{CP} is not populated by pairs that demonstrate the similarities or relations of classes. If the classifier is trained to remedy its weakness in real time from the beginning, estimated confusion distribution will not reflect the underlying relationships of classes. To remedy these problems, we design CP-Mix training to follow ERM training, where \mathcal{CP} is collected during the whole training time, but mixup regularization with confusion pairs works at the second stage. By doing so, we not only populate \mathcal{CP} with pairs that the ERM classifier confuses but also reduce the computational overhead during training.

We construct a mini-batch for CP-Mix in the following steps given the multiset \mathcal{CP} , as shown in Algorithm 1. First, we sample a set of B' classes $\{(c_{b,t})\}_{b=0}^{B'-1}$ uniformly from the label set $\mathcal{C} = \{0, \dots, C-1\}$ where B' is a batch size for mixup. This sampling does not consider class distribution in confusion-pairs \mathcal{CP} since it is imbalanced due to the source training set's imbalance. Then we sample a pair of classes $(c_{b,t}, c_{b,m})$ for each $c_{b,t}$ where $c_{b,m}$ is sampled from a subset $\{(c_t, c_m) | (c_t, c_m) \in \mathcal{CP}, c_t = c_{b,t}\}$. After we obtain a set of B' confusion-pairs $\{(c_{b,t}, c_{b,m})\}_{b=0}^{B'-1}$, we sample $x_{b,t}$ and $x_{b,m}$ from the subsets $\mathcal{D}_{c_{b,t}}$ and $\mathcal{D}_{c_{b,m}}$ for each confusion pair $(c_{b,t}, c_{b,m})$. Finally, we perform pairwise mixing of $x_{b,t}$ and $x_{b,m}$ using the mixing functions proposed in Section 4.2.

Combining the above proposals, CP-Mix objective is

$$\mathcal{L}_{CP}(\theta, l) = \mathbb{E}_{(\tilde{x}, \tilde{y}) \sim \tilde{\mathcal{P}}_{CP}} [l(f_\theta(\tilde{x}), \tilde{y})] \approx \frac{1}{N''} \sum_{(\tilde{x}_i, \tilde{y}_i) \in \tilde{\mathcal{D}}_{s, CP}} l(f_\theta(\tilde{x}_i), \tilde{y}_i), \quad (11)$$

²It can be replaced by counting actual confusion values $C_{i,j}$, but we use the concept of multiset for easier understanding.

Algorithm 1: CP-Mix

Input: $f_\theta, \mathcal{D}_s = \{(x_i, y_i)\}_{i=0}^{N-1}$
Hyperparameter: E, E_{cp}, B, B', γ ;
Initialize f_θ , Confusion-pairs $\mathcal{CP} \leftarrow []$;
for $e = 1$ **to** E **do**
 foreach batch $\mathcal{B} = \{(x_i, y_i)\}_{i=0}^{B-1} \in \mathcal{D}_s$ **do**
 $\mathcal{L}(\theta) \leftarrow \mathcal{L}_{ERM}(\theta, l_{ERM})$ using \mathcal{B} ;
 Get predictions $P = \{(x_i, y_i, y_{i,p})\}_{i=0}^{B-1}$;
 Append misclassifications $[(y_i, y_{i,p}) \mid (x_i, y_i, y_{i,p}) \in P, y_i \neq y_{i,p}]$ to \mathcal{CP} ;
 if $e > E_{cp}$ **then**
 Sample classes $\{(c_{b,t})\}_{b=0}^{B'-1}$ uniformly from \mathcal{C} ;
 Sample confusion-pairs $\{(c_{b,t}, c_{b,m})\}_{b=0}^{B'-1}$ from \mathcal{CP} given $\{(c_{b,t})\}_{b=0}^{B'-1}$;
 Sample batch $\mathcal{B}_{CP} = \{((x_{b,t}, c_{b,t}), (x_{b,m}, c_{b,m}))\}_{b=0}^{B'-1}$ from \mathcal{D}_s ;
 Mix samples in \mathcal{B}_{CP} and compute $\mathcal{L}_{CP}(\theta, l_{CP})$;
 $\mathcal{L}(\theta) \leftarrow \mathcal{L}(\theta) + \gamma \times \mathcal{L}_{CP}(\theta, l_{CP})$;
 Update θ using $\mathcal{L}(\theta)$;
Output: f_θ

where $\tilde{\mathcal{P}}_{CP}$ is a CP-mixed data distribution and $\tilde{\mathcal{D}}_{s,CP}$ is a set of CP-mixed examples with N'' cardinality. As discussed, a mini-batch \mathcal{B}_{CP} for mixup is sampled based on confusion-pairs.

We obtain the overall objective as

$$\mathcal{L}(\theta) = \mathcal{L}_{ERM}(\theta, l_{ERM}) + \gamma \mathcal{L}_{CP}(\theta, l_{CP}), \quad (12)$$

where γ is a hyper-parameter. We use balanced softmax [50] for l_{ERM} and cross-entropy loss for l_{CP} , considering underlying data distribution for these objectives.³ In practice, we apply additional mixup regularization with cross-entropy loss using the imbalanced training set to stabilize the training. More details can be found in Appendix A.

5 Experiments

In this section, we first provide the experimental settings to evaluate how CP-Mix works when the training set is severely imbalanced. Then, we demonstrate that CP-Mix outperforms existing state-of-the-art methods across multiple long-tailed datasets. This is followed by a detailed ablation study that dissects the various components contributing to the performance improvement of CP-Mix.

5.1 Experimental settings

Datasets and model architecture We use five datasets commonly benchmarked for long-tailed image recognition (*i.e.*, two CIFAR-LT [30], ImageNet-LT [51], Places-LT [51], and iNaturalist 2018 [52]). CIFAR-LT are artificial versions of CIFAR10 and CIFAR100 datasets [53] with exponential class imbalance factors varying from 10 to 200. ImageNet-LT and Places-LT are long-tailed versions of real-world datasets ImageNet [1] and Places [54], and we follow the standard procedure to build these datasets. iNaturalist 2018 is a large-scale real-world dataset with an imbalanced distribution. For a fair comparison, we follow previous works about network architecture. More information about the datasets and model architectures is summarized in Appendix B.2.

Evaluation protocols We use the uniform test set to evaluate methods and report the top-1 accuracy. Following [51], we also report the accuracy evaluated on three disjoint class subgroups divided according to the number of training examples in each class (*i.e.* many (more than 100), medium (from 20 to 100), and few (less than 20) shots) for large-scale datasets in Appendix C.

Baselines We compare CP-Mix with various representative approaches for long-tailed image classification. They are categorized into **a) Loss modification** (Balanced Softmax [50] and LADE [35], including Cross Entropy as baseline),

³The data distribution for l_{CP} already considers the imbalance and model's bias, while the data distribution for l_{ERM} is imbalanced.

Dataset	CIFAR100-LT				CIFAR10-LT			
Imbalance factor ρ	200	100	50	10	200	100	50	10
Cross Entropy [†]	34.84	38.32	43.26	57.00	65.68	70.36	77.10	86.89
LDAM-DRW [†]	39.03	43.64	47.31	56.90	76.14	79.58	82.96	87.48
Balanced Softmax [†]	38.01	42.71	46.68	58.34	74.48	77.20	81.26	87.46
MiSLAS	—	47.0	52.3	63.2	—	82.1	85.7	90.0
Remix	36.99	41.94	46.21	59.36	—	79.76	—	89.02
CMO	—	43.9	48.3	59.5	—	—	—	—
UniMix	42.07	45.45	51.11	61.25	78.48	82.75	84.32	89.66
OTmix (BS)	—	46.8	52.3	62.3	—	84.0	86.5	90.2
ACE	—	49.6	51.9	—	—	81.4	84.9	—
RIDE [†]	46.34	49.83	52.73	59.30	79.16	82.31	84.61	87.19
CMO+RIDE	—	50.0	53.0	60.2	—	—	—	—
SADE	—	49.8	53.9	63.6	—	—	—	—
OTMix+RIDE	—	50.7	53.8	60.8	—	82.7	85.2	88.7
CP-Mix [†]	43.56	48.20	52.12	61.91	78.34	82.44	85.08	89.87
CP-Mix + RIDE [†]	47.37	51.40	55.77	62.17	79.67	81.56	84.23	86.70

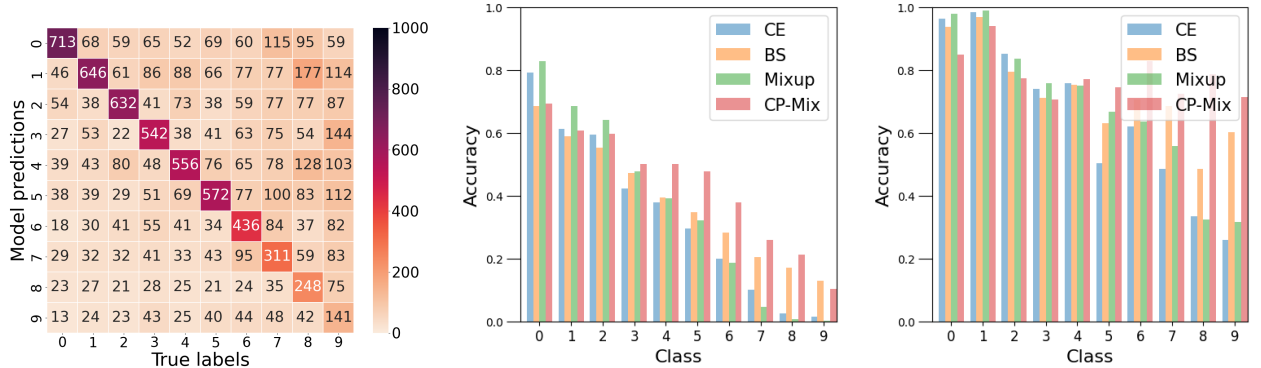
Table 1: Experimental results for CIFAR-LT datasets. [†] denotes results reproduced by us, and others are from the original papers. **The advantages of the proposed CP-Mix are highlighted as the task becomes challenging, especially for CIFAR100-LT with large imbalance factors.** CP-Mix is compatible with ensemble-based methods, outperforming other ensemble-based methods for challenging tasks.

Dataset	ImageNet-LT	Places-LT	iNaturalist 2018
Cross Entropy [†]	45.5	32.3	64.5
Balanced Softmax [†]	50.6	39.3	69.9
LADE	—	39.2	69.3
LDAM-DRW [†]	50.3	—	66.9
MiSLAS	52.7	40.4	71.6
Remix	48.6	—	70.5
UniMix	48.6	—	70.5
OTmix (BS)	55.6	—	71.5
ACE	54.7	—	72.9
RIDE [†]	55.4	40.3	72.6
CMO+RIDE	56.2	—	72.8
SADE	—	40.9	72.9
OTmix+RIDE	57.3	—	73.0
CP-Mix	53.9	42.3	72.3
CP-Mix+RIDE	56.6	—	73.7

Table 2: Results for large-scale datasets. [†] denotes results reproduced by us, and others are from the original papers. CP-Mix performs better when the number of categories and imbalance factor increase (iNaturalist 2018), demonstrating its superiority in tackling challenging problems.

b) Two-stage methods (LDAM-DRW [32] and MiSLAS [21]), and **c) Mixup and generation methods** (Remix [19], CMO [22], UniMix [46] and OTmix [24]). We also include **d) Ensemble-based methods** (RIDE [39], ACE [40], and SADE [42]) to evaluate the performance of CP-Mix combined with RIDE.

Implementation details We follow the common practices for implementation details from the literature. We trained the models using SGD optimizer with momentum 0.9. The learning rate for the training is 0.1, except for the Places-LT, which uses 0.01. We finetune the models using the class-balanced training dataset following the method proposed in [55]. More details about training and hyper-parameters for CP-Mix can be found in Appendix B.3.



(a) Confusion matrix of CP-Mix classifier on CIFAR100-LT-200 dataset.

(b) Class-wise accuracy on CIFAR100-LT-200 dataset.

(c) Class-wise accuracy on CIFAR10-LT200 dataset.

Figure 4: (a) Confusion matrix of the CP-Mix classifier trained on CIFAR100-LT-200 dataset. **It successfully reduces high confusion in the upper right region by sacrificing low confusion in the lower left region, which indicates the number of majorities misclassified as minorities.** This results in more balanced accuracies among categories. (b, c) Class-wise accuracy of the classifiers trained on CIFAR100-LT-200 and CIFAR10-LT-200 datasets. **CP-Mix significantly improves the accuracies on minority classes, resulting in more balanced sub-group accuracies.**

5.2 Long-tailed image classification

We evaluate CP-Mix on famous long-tailed classification datasets (CIFAR-LT with varying imbalance factors from 200 to 10, and three large-scale datasets). Experimental results for CIFAR-LT and large-scale datasets are reported in Table 1 and 2, respectively. The superiority of CP-Mix is highlighted for the complex tasks like CIFAR100-LT with imbalance factors of 200 and 100 or large-scale datasets while achieving comparable performance on smaller or less-imbalanced datasets. We also augment CP-Mix with RIDE to demonstrate its compatibility with ensemble-based method, and it outperforms other ensemble-based methods (ACE, RIDE and SADE). Notably, ensemble-based methods cannot outperform simple methods when imbalance ratio is not significant or the number of categories is not large. Additional results on three disjoint subgroups of categories are reported in Appendix C.1. CP-Mix is better at achieving trade-offs between sub-group performances. This implies that mixup is ineffective for large-scale images if we do not consider the imbalance and confusion.

OTmix [24] is the most relevant work that combines mixup with a confusion matrix. While it utilizes mixup to augment its proposed method based on optimal transport, CP-Mix has an important difference from OTmix. CP-Mix is carefully designed to reveal the model’s confusion in real-time without having a balanced validation set, which is more practical in a real-world scenario. However, OTmix uses the balanced validation set to obtain the confusions of the model. This implies that our CP-Mix is more practical in tackling long-tailed problems.

5.3 Analysis of CP-Mix

We conduct further analysis to understand the advantages of CP-Mix. Our experiments aim to answer the following questions: 1) Can CP-Mix alleviate confusion-pairs? 2) How does it improve class-wise performance? and 3) What compositions of CP-Mix boost long-tailed recognition? All study in this subsection is conducted on the classifiers trained on CIFAR100-LT dataset with the imbalance factor $\rho = 200$ if not specified.

5.3.1 Confusion matrix

CP-Mix utilizes the confusion-pairs as a clue of the model’s weakness and augments samples between these pairs to relieve confusions. We compare the confusion matrix of CP-Mix to that of ERM and Mixup classifiers to demonstrate that CP-Mix successfully relieves confusions of the model while Mixup cannot. Figure 4(a) illustrates the model’s weakness in misclassifying minorities to similar counterparts, showing its enhanced generalization to minority classes. On the other hand, confusion matrices in Figure 3 demonstrate the clear tendency between the true classes and mispredictions. This implies that CP-Mix can capture the confusion distribution of the classifier, and sampling from the confusion-pairs is beneficial in relieving the confusion. Also, the diagonals of the matrices demonstrate class-wise accuracy, and CP-Mix achieves a fairer class-wise performance by improving accuracy on minority classes. More confusion matrices on different datasets are provided in Appendix C.2.

l_{ERM}	Mixup Reg	Mixing functions	Confusion-pairs	Additional Reg	Finetuning	Top-1 accuracy
CE	×	—	—	—	—	34.84
BS	×	—	—	—	—	38.01
BS	✓	×	×	—	—	36.48
BS	✓	✓	×	—	—	37.21
BS	✓	×	✓	—	—	41.28
BS	✓	×	✓	✓	—	41.26
BS	✓	✓	✓	—	—	40.26
BS	✓	✓	✓	✓	×	42.77
BS	✓	✓	✓	✓	✓	43.56 (CP-Mix)

Table 3: Ablation study to analyze the components of CP-Mix on CIFAR100-LT200 dataset. CE and BS denote Cross Entropy and Balanced Softmax, respectively.

l_{ERM}	Mixup Reg	Mixing functions	Confusion-pairs	Additional Reg	Finetuning	Top-1 accuracy
CE	×	—	—	—	—	45.5
BS	×	—	—	—	—	50.6
BS	✓	×	×	—	—	46.8
BS	✓	✓	×	—	—	48.9
BS	✓	×	✓	—	—	51.8
BS	✓	×	✓	✓	—	51.9
BS	✓	✓	✓	—	—	52.3
BS	✓	✓	✓	✓	×	52.9
BS	✓	✓	✓	✓	✓	53.9 (CP-Mix)

Table 4: Ablation study to analyze the components of CP-Mix on ImageNet-LT dataset. CE and BS denote Cross Entropy and Balanced Softmax, respectively.

5.3.2 Class-wise accuracy

Figure 4(b) and (c) compare the class-wise accuracy of the models trained on CIFAR100-LT-200 and CIFAR10-LT-200 datasets. We group adjacent classes into 10 subgroups for visualization of CIFAR100-LT dataset. CP-Mix boosts the performance of minorities by a large margin while sacrificing the performance of majorities little. Balanced softmax, which considers the imbalance and achieves trade-offs between majorities and minorities, demonstrates much lower benefits. As analyzed in Section 3.2, Mixup improves generalization in majorities by sacrificing minority groups, resulting in a more biased classifier.

5.3.3 Ablation study

We analyze what components of CP-Mix lead to the performance boost in long-tailed image recognition. Table 3 and 4 present the effects of different components to the performance of CP-Mix for CIFAR100-LT-200 and ImageNet-LT datasets, respectively. First, it is evident that balanced softmax [50] is a strong baseline that improves cross-entropy by a large margin. Using Mixup regularization and revising mixup formulation to consider imbalance cannot achieve the improvements. By estimating confusion distribution and using confusion-pairs for mixup regularization, we can improve the classifiers by a large margin. Using mixing functions proposed in Section 4.2 has limitations but is stabilized with additional regularization, achieving the best performance.

6 Conclusion

This paper proposes CP-Mix, a novel training framework using mixup to tackle long-tailed recognition. Inspired by model’s tendency to capture class similarities and misclassify minorities to similar majorities, we propose to collect confusion-pairs to augment samples by mixing from these classes. Our method trains the model to reduce confusion by regularizing to distinguish confusing classes. We demonstrate the superiority and compatibility of CP-Mix in

various long-tailed image classification benchmarks. Moreover, we analyze CP-Mix and reveal how CP-Mix works and improves classification. Our work suggests the possibility of Mixup to improve more complex computer vision tasks.

References

- [1] Jia Deng, Wei Dong, Richard Socher, Li-Jia Li, Kai Li, and Li Fei-Fei. Imagenet: A large-scale hierarchical image database. In *2009 IEEE Conference on Computer Vision and Pattern Recognition*, pages 248–255, 2009.
- [2] Tal Ridnik, Emanuel Ben-Baruch, Asaf Noy, and Lihi Zelnik-Manor. Imagenet-21k pretraining for the masses. 2021.
- [3] Diederik P Kingma and Jimmy Ba. Adam: A method for stochastic optimization. *arXiv preprint arXiv:1412.6980*, 2014.
- [4] Sergey Ioffe and Christian Szegedy. Batch normalization: Accelerating deep network training by reducing internal covariate shift. In *International conference on machine learning*, pages 448–456. pmlr, 2015.
- [5] Kaiming He, Xiangyu Zhang, Shaoqing Ren, and Jian Sun. Deep residual learning for image recognition. In *Proceedings of the IEEE conference on computer vision and pattern recognition*, pages 770–778, 2016.
- [6] Alexey Dosovitskiy, Lucas Beyer, Alexander Kolesnikov, Dirk Weissenborn, Xiaohua Zhai, Thomas Unterthiner, Mostafa Dehghani, Matthias Minderer, Georg Heigold, Sylvain Gelly, et al. An image is worth 16x16 words: Transformers for image recognition at scale. *arXiv preprint arXiv:2010.11929*, 2020.
- [7] Nitesh V Chawla, Kevin W Bowyer, Lawrence O Hall, and W Philip Kegelmeyer. Smote: synthetic minority over-sampling technique. *Journal of artificial intelligence research*, 16:321–357, 2002.
- [8] Felix Last, Georgios Douzas, and Fernando Bacao. Oversampling for imbalanced learning based on k-means and smote. *arXiv preprint arXiv:1711.00837*, 2017.
- [9] Jaehyung Kim, Jongheon Jeong, and Jinwoo Shin. M2m: Imbalanced classification via major-to-minor translation. In *Proceedings of the IEEE/CVF conference on computer vision and pattern recognition*, pages 13896–13905, 2020.
- [10] Hongyi Zhang, Moustapha Cisse, Yann N. Dauphin, and David Lopez-Paz. mixup: Beyond empirical risk minimization. In *International Conference on Learning Representations*, 2018.
- [11] Vikas Verma, Alex Lamb, Christopher Beckham, Amir Najafi, Aaron Courville, Ioannis Mitliagkas, and Yoshua Bengio. Manifold mixup: Learning better representations by interpolating hidden states, 2019.
- [12] Sangdoo Yun, Dongyoon Han, Seong Joon Oh, Sanghyuk Chun, Junsuk Choe, and Youngjoon Yoo. Cutmix: Regularization strategy to train strong classifiers with localizable features. In *Proceedings of the IEEE/CVF International Conference on Computer Vision (ICCV)*, October 2019.
- [13] Dan Hendrycks*, Norman Mu*, Ekin Dogus Cubuk, Barret Zoph, Justin Gilmer, and Balaji Lakshminarayanan. Augmix: A simple method to improve robustness and uncertainty under data shift. In *International Conference on Learning Representations*, 2020.
- [14] JangHyun Kim, Wonho Choo, Hosan Jeong, and Hyun Oh Song. Co-mixup: Saliency guided joint mixup with supermodular diversity. In *International Conference on Learning Representations*, 2021.
- [15] Jang-Hyun Kim, Wonho Choo, and Hyun Oh Song. Puzzle mix: Exploiting saliency and local statistics for optimal mixup. In *International Conference on Machine Learning*, pages 5275–5285. PMLR, 2020.
- [16] Jy-Yong Sohn, Liang Shang, Hongxu Chen, Jaekyun Moon, Dimitris Papailiopoulos, and Kangwook Lee. Genlabel: Mixup relabeling using generative models. In *International Conference on Machine Learning*, pages 20278–20313. PMLR, 2022.
- [17] AFM Shahab Uddin, Mst Sirazam Monira, Wheemyung Shin, TaeChoong Chung, and Sung-Ho Bae. Saliencymix: A saliency guided data augmentation strategy for better regularization. In *International Conference on Learning Representations*.
- [18] Sangwoo Hong, Youngseok Yoon, Hyungjun Joo, and Jungwoo Lee. Gbmix: Enhancing fairness by group-balanced mixup. *IEEE Access*, pages 1–1, 2024.
- [19] Hsin-Ping Chou, Shih-Chieh Chang, Jia-Yu Pan, Wei Wei, and Da-Cheng Juan. Remix: rebalanced mixup. In *Computer Vision–ECCV 2020 Workshops: Glasgow, UK, August 23–28, 2020, Proceedings, Part VI 16*, pages 95–110. Springer, 2020.
- [20] Anubha Kabra, Ayush Chopra, Nikaash Puri, Pinkesh Badjatiya, Sukriti Verma, Piyush Gupta, et al. Mixboost: Synthetic oversampling with boosted mixup for handling extreme imbalance. *arXiv preprint arXiv:2009.01571*, 2020.
- [21] Zhisheng Zhong, Jiequan Cui, Shu Liu, and Jiaya Jia. Improving calibration for long-tailed recognition. In *Proceedings of the IEEE/CVF conference on computer vision and pattern recognition*, pages 16489–16498, 2021.
- [22] Seulki Park, Youngkyu Hong, Byeongho Heo, Sangdoo Yun, and Jin Young Choi. The majority can help the minority: Context-rich minority oversampling for long-tailed classification. In *Proceedings of the IEEE/CVF Conference on Computer Vision and Pattern Recognition*, pages 6887–6896, 2022.
- [23] Jiang-Xin Shi, Tong Wei, Yuke Xiang, and Yu-Feng Li. How re-sampling helps for long-tail learning? *arXiv preprint arXiv:2310.18236*, 2023.
- [24] Jintong Gao, He Zhao, Zhuo Li, and Dan dan Guo. Enhancing minority classes by mixing: An adaptative optimal transport approach for long-tailed classification. In *Thirty-seventh Conference on Neural Information Processing Systems*, 2023.

- [25] Zhi-Hua Zhou and Xu-Ying Liu. Training cost-sensitive neural networks with methods addressing the class imbalance problem. *IEEE Transactions on Knowledge and Data Engineering*, 18(1):63–77, 2006.
- [26] Show-Jane Yen and Yue-Shi Lee. Cluster-based under-sampling approaches for imbalanced data distributions. *Expert Systems with Applications*, 36(3, Part 1):5718–5727, 2009.
- [27] Chen Huang, Yining Li, Chen Change Loy, and Xiaoou Tang. Learning deep representation for imbalanced classification. In *Proceedings of the IEEE Conference on Computer Vision and Pattern Recognition (CVPR)*, June 2016.
- [28] Yu-Xiong Wang, Deva Ramanan, and Martial Hebert. Learning to model the tail. In *Advances in Neural Information Processing Systems*, volume 30, 2017.
- [29] Mateusz Buda, Atsuto Maki, and Maciej A. Mazurowski. A systematic study of the class imbalance problem in convolutional neural networks. *Neural Networks*, 106:249–259, 2018.
- [30] Yin Cui, Menglin Jia, Tsung-Yi Lin, Yang Song, and Serge Belongie. Class-balanced loss based on effective number of samples. In *Proceedings of the IEEE/CVF Conference on Computer Vision and Pattern Recognition (CVPR)*, June 2019.
- [31] Tsung-Yi Lin, Priya Goyal, Ross Girshick, Kaiming He, and Piotr Dollár. Focal loss for dense object detection. In *Proceedings of the IEEE international conference on computer vision*, pages 2980–2988, 2017.
- [32] Kaidi Cao, Colin Wei, Adrien Gaidon, Nikos Arechiga, and Tengyu Ma. Learning imbalanced datasets with label-distribution-aware margin loss. *Advances in neural information processing systems*, 32, 2019.
- [33] Saptarshi Sinha, Hiroki Ohashi, and Katsuyuki Nakamura. Class-wise difficulty-balanced loss for solving class-imbalance. In *Proceedings of the Asian conference on computer vision*, 2020.
- [34] Jingru Tan, Changbao Wang, Buyu Li, Quanquan Li, Wanli Ouyang, Changqing Yin, and Junjie Yan. Equalization loss for long-tailed object recognition. In *Proceedings of the IEEE/CVF conference on computer vision and pattern recognition*, pages 11662–11671, 2020.
- [35] Youngkyu Hong, Seungju Han, Kwanghee Choi, Seokjun Seo, Beomsu Kim, and Buru Chang. Disentangling label distribution for long-tailed visual recognition. In *Proceedings of the IEEE/CVF conference on computer vision and pattern recognition*, pages 6626–6636, 2021.
- [36] Zitai Wang, Qianqian Xu, Zhiyong Yang, Yuan He, Xiaochun Cao, and Qingming Huang. A unified generalization analysis of re-weighting and logit-adjustment for imbalanced learning. *arXiv preprint arXiv:2310.04752*, 2023.
- [37] Boyan Zhou, Quan Cui, Xiu-Shen Wei, and Zhao-Min Chen. Bbn: Bilateral-branch network with cumulative learning for long-tailed visual recognition. In *Proceedings of the IEEE/CVF conference on computer vision and pattern recognition*, pages 9719–9728, 2020.
- [38] Liuyu Xiang, Guiguang Ding, and Jungong Han. Learning from multiple experts: Self-paced knowledge distillation for long-tailed classification. In *Computer Vision–ECCV 2020: 16th European Conference, Glasgow, UK, August 23–28, 2020, Proceedings, Part V 16*, pages 247–263. Springer, 2020.
- [39] Xudong Wang, Long Lian, Zhongqi Miao, Ziwei Liu, and Stella X Yu. Long-tailed recognition by routing diverse distribution-aware experts. *arXiv preprint arXiv:2010.01809*, 2020.
- [40] Jiarui Cai, Yizhou Wang, and Jenq-Neng Hwang. Ace: Ally complementary experts for solving long-tailed recognition in one-shot. In *Proceedings of the IEEE/CVF International Conference on Computer Vision*, pages 112–121, 2021.
- [41] Jun Li, Zichang Tan, Jun Wan, Zhen Lei, and Guodong Guo. Nested collaborative learning for long-tailed visual recognition. In *Proceedings of the IEEE/CVF Conference on Computer Vision and Pattern Recognition*, pages 6949–6958, 2022.
- [42] Yifan Zhang, Bryan Hooi, Lanqing Hong, and Jiashi Feng. Self-supervised aggregation of diverse experts for test-agnostic long-tailed recognition. *Advances in Neural Information Processing Systems*, 35:34077–34090, 2022.
- [43] Olivier Chapelle, Jason Weston, Léon Bottou, and Vladimir Vapnik. Vicinal risk minimization. *Advances in neural information processing systems*, 13, 2000.
- [44] Muthu Chidambaram, Xiang Wang, Yuzheng Hu, Chenwei Wu, and Rong Ge. Towards understanding the data dependency of mixup-style training. *arXiv preprint arXiv:2110.07647*, 2021.
- [45] Hongyu Guo, Yongyi Mao, and Richong Zhang. Mixup as locally linear out-of-manifold regularization. AAAI’19/IAAI’19/EAAI’19. AAAI Press, 2019.
- [46] Zhengzhuo Xu, Zenghao Chai, and Chun Yuan. Towards calibrated model for long-tailed visual recognition from prior perspective. *Advances in Neural Information Processing Systems*, 34:7139–7152, 2021.
- [47] L Zhang, Z Deng, K Kawaguchi, A Ghorbani, and J Zou. How does mixup help with robustness and generalization? In *International Conference on Learning Representations*, 2021.
- [48] Francesco Pinto, Harry Yang, Ser-Nam Lim, Philip HS Torr, and Puneet K Dokania. Regmixup: Mixup as a regularizer can surprisingly improve accuracy and out distribution robustness. *arXiv preprint arXiv:2206.14502*, 2022.
- [49] Yongshun Zhang, Xiu-Shen Wei, Boyan Zhou, and Jianxin Wu. Bag of tricks for long-tailed visual recognition with deep convolutional neural networks. In *Proceedings of the AAAI conference on artificial intelligence*, volume 35, pages 3447–3455, 2021.

- [50] Jiawei Ren, Cunjun Yu, Xiao Ma, Haiyu Zhao, Shuai Yi, et al. Balanced meta-softmax for long-tailed visual recognition. *Advances in neural information processing systems*, 33:4175–4186, 2020.
- [51] Ziwei Liu, Zhongqi Miao, Xiaohang Zhan, Jiayun Wang, Boqing Gong, and Stella X Yu. Large-scale long-tailed recognition in an open world. In *Proceedings of the IEEE/CVF conference on computer vision and pattern recognition*, pages 2537–2546, 2019.
- [52] Grant Van Horn, Oisin Mac Aodha, Yang Song, Yin Cui, Chen Sun, Alex Shepard, Hartwig Adam, Pietro Perona, and Serge Belongie. The inaturalist species classification and detection dataset. In *Proceedings of the IEEE conference on computer vision and pattern recognition*, pages 8769–8778, 2018.
- [53] Alex Krizhevsky, Geoffrey Hinton, et al. Learning multiple layers of features from tiny images. 2009.
- [54] Bolei Zhou, Agata Lapedriza, Aditya Khosla, Aude Oliva, and Antonio Torralba. Places: A 10 million image database for scene recognition. *IEEE Transactions on Pattern Analysis and Machine Intelligence*, 40(6):1452–1464, 2018.
- [55] Puja Trivedi, Danai Koutra, and Jayaraman J Thiagarajan. A closer look at model adaptation using feature distortion and simplicity bias. *arXiv preprint arXiv:2303.13500*, 2023.

Appendix

A Objective function.

CP-Mix augments the objective for ERM training with a regularization objective using confusion pairs. As mentioned in the main paper, we use an additional mixup regularization objective using the same training batch for classification to stabilize the training following RegMix. We use the same mixup hyperparameter α and regularization ratio γ to reduce the search space for training hyperparameters. The overall objective for CP-Mix is

$$\mathcal{L}(\theta) = \mathcal{L}_{ERM}(\theta, l_{ERM}) + \gamma_{CP} \mathcal{L}_{CP}(\theta, l_{CP}) + \gamma_{mix} \mathcal{L}_{mix}(\theta, l_{mix}), \quad (13)$$

where

$$\mathcal{L}_{ERM}(\theta, l_{ERM}) = \mathbb{E}_{(x,y) \sim \mathcal{P}}[l_{ERM}(f_{\theta}(x), y)] \approx \frac{1}{N} \sum_{(x_i, y_i) \in \mathcal{D}_s} l_{ERM}(f_{\theta}(x_i), y_i), \quad (14)$$

$$\mathcal{L}_{CP}(\theta, l_{CP}) = \mathbb{E}_{(\tilde{x}, \tilde{y}) \sim \tilde{\mathcal{P}}_{CP}}[l_{CP}(f_{\theta}(\tilde{x}), \tilde{y})] \approx \frac{1}{N''} \sum_{(\tilde{x}_i, \tilde{y}_i) \in \tilde{\mathcal{D}}_{s, CP}} l_{CP}(f_{\theta}(\tilde{x}_i), \tilde{y}_i), \quad (15)$$

$$\mathcal{L}_{mix}(\theta, l_{mix}) = \mathbb{E}_{(\tilde{x}, \tilde{y}) \sim \tilde{\mathcal{P}}} [l_{mix}(f_{\theta}(\tilde{x}), \tilde{y})] \approx \frac{1}{N'} \sum_{(\tilde{x}_i, \tilde{y}_i) \in \tilde{\mathcal{D}}_s} l_{mix}(f_{\theta}(\tilde{x}_i), \tilde{y}_i). \quad (16)$$

and Balanced Softmax is used for l_{ERM} , and Cross-Entropy is used for l_{CP} and l_{mix} . $\tilde{\mathcal{D}}_s$ is constructed using the same batch to that of \mathcal{D}_s , and $\tilde{\mathcal{D}}_{s, CP}$ is sampled using the class-wise subsets and confusion pairs. CP-Mix utilizes the same mixup strategy for both CP-Mix and regularization objectives.

B Implementation details

B.1 Toy example

We use a 2D example to demonstrate how a decision boundary is constructed, and Mixup fails to improve minority generalization. There are 4 classes where data points are sampled from the Gaussian distributions. The centers for majorities are $(0, 1)$ and $(1, 0)$, and are $(0, -1)$ and $(-1, 0)$ for minorities. The standard deviation is 0.4 for all classes, and 1,000 and 50 training points are sampled for majorities and minorities, respectively. We sampled 1,000 points for the test set from each class. The classifier is a fully connected network with one hidden layer containing 100 nodes (two linear modules), and the ReLU function is used for activation. Adam optimizer is used, and the classifier is trained for 10 epochs with a learning rate of 0.1 and batch size of 100.

B.2 Datasets and architecture

This subsection presents the details of datasets and network architectures we use to evaluate CP-Mix. We follow the standard process to construct imbalanced datasets. The information is summarized in Table 5.

Dataset	# of classes	# of training samples	Imbalance factor	Architecture
CIFAR-LT	100/10	50,000	[10, 50, 100, 200]	ResNet-32
ImageNet-LT	1,000	115,846	256	ResNet-50
Places-LT	365	62,500	996	Pre-trained ResNet-152
iNaturalist 2018	8,124	427,513	500	ResNet-50

Table 5: Detailed information of datasets and architecture. Our choices for model architecture are based on previous works.

B.2.1 CIFAR-LT

CIFAR-LT datasets are the artificially imbalanced version of CIFAR datasets with exponential class imbalance. Specifically, the number of training examples in class i is reduced according to an exponential function as $n_i = n_0 \mu^i$, and the imbalance factor of the dataset is $\rho = \frac{n_0}{n_{C-1}} = \mu^{-C+1}$. We conduct experiments for CIFAR100-LT and CIFAR10-LT datasets with an imbalance factor in [200, 100, 50, 10]. A general augmentation strategy with random crop and random horizontal flip is used after 4 pixels padding for the comparison. Following previous works, we use ResNet-32 architecture for CIFAR-LT datasets.

	CIFAR-LT	ImageNet-LT	Places-LT	iNaturalist 2018
batch size	128	192	128	256
max epochs	300	180	30	100
stage 1 epochs	200	120	15	50
stage 2 epochs	100	60	15	50
optimizer	SGD	SGD	SGD	SGD
learning rate	0.1	0.1	0.01	0.1
momentum	0.9	0.9	0.9	0.9
weight decay	0.0002	0.0005	0.0005	0.0002
scheduler	warmup multistep	cosine	multistep	warmup multistep
steps	[260, 280]	—	[5, 15]	[60, 80]
decay rate	0.01	—	0.1	0.1
t	0.5	0.5	0.5	0.5
$\alpha = \alpha_{CP} = \alpha_{mix}$	1.5	3.0	1.0	1.0
$\gamma = \gamma_{CP} = \gamma_{mix}$	2.5	1.0	2.0	1.0
fine-tuning epochs	30	10	—	10
fine-tuning lr	0.5, 0.1	0.05	—	3.0
fine-tuning momentum	0.9	0.9	—	0.9
fine-tuning weight decay	0.0	0.0	—	0.0

Table 6: Hyperparameter settings for experimental results. We provide more details and settings about RIDE training in the text.

B.2.2 ImageNet-LT

ImageNet-LT is sampled from ImageNet dataset under the long-tailed Pareto distribution with power value $\alpha = 6$. It contains 115.8K examples from 1,000 classes with the largest and smallest class size 1,260 and 5, respectively ($\rho = 256$). Examples are resized to 256×256 , and random crop, random horizontal flip, and color jitter are used for data augmentation. We use ResNet-50 architecture for this large-scale dataset following previous works.

B.2.3 Places-LT

Places-LT is an imbalanced dataset sampled from a large-scale Places dataset following a strategy similar to ImageNet-LT. It comprises 184.5K examples from 365 classes with the largest and smallest class size 4,980 and 5 ($\rho = 996$). The same pre-processing is used with ImageNet-LT. Following the previous works, we use ResNet-152 architecture pre-trained using ImageNet.

B.2.4 iNaturalist 2018

iNaturalist 2018 dataset is a species classification benchmark with a natural long-tailed class distribution. It contains 437.5K examples from 8,142 classes with the fine-grained hierarchy. The largest classes have 1,000 examples, while the smallest has only 2. We use ResNet-50 architecture with a normed layer for the classifier following the literature. We note that a normed layer contributes significantly to the baseline performance.

B.3 Training details

This subsection details the implementations and hyperparameters for the main results and analysis. Our experiment results are divided into two parts: base results and RIDE results. Training details mainly follow previous works for base results, except for the longer training of CIFAR-LT and ImageNet-LT experiments due to additional regularization. We reduce the batch size if necessary since mixup regularization requires additional memory usage. For RIDE results, we strictly follow the settings from the original paper for a fair comparison. We note that RIDE uses a deferred reweighting strategy, and we use six experts for all cases. Also, we did not fine-tune the classifier for RIDE results. Basic hyperparameter settings for base results are summarized in Table 6, and we detail more specifics and RIDE training settings in the following subsections.

CP-Mix is a two-stage training framework where the first one is similar to the ERM training, and the second stage involves Mixup regularization using confusion-pairs. The only difference between our first stage and ERM training is that CP-Mix should collect confusion-pairs from the training phase. Generally, two over three of the whole training time is stage 1, and one over three is for stage 2.

B.3.1 CIFAR-LT

We train the model for 300 epochs with CP-Mix regularization for the last 100 epochs and a learning rate decays at 260 and 280 epochs with 10 warmup epochs warmup. For base results, we finetune the models with the backbone frozen for the 30 epochs. The learning rate for finetuning is 0.5 for CIFAR100-LT datasets and 0.1 for CIFAR10-LT datasets. For RIDE training, we train the model for 200 epochs using a normed layer for the classifier, Nesterov momentum for SGD optimizer, and 0.0005 for weight decay, following the original paper. We do not finetune the models for RIDE results.

B.3.2 ImageNet-LT

We use cosine annealing for base results and train the models for 180 epochs. After that, we finetune the classifier for 10 epochs with the feature extractor frozen. The learning rate is 0.5 for finetuning. Following the original implementation, we train the RIDE models for 100 epochs with multistep scheduling at 60 and 80 epochs with a linear warmup for 5 epochs.

B.3.3 Places-LT

We train the pre-trained model for 30 epochs with the learning rate decayed at 5 and 15 epochs by 0.1, starting from 0.01. We do not fine-tune the classifier for Places-LT dataset.

B.3.4 iNaturalist 2018

Following the previous works, we use ResNet-50 architecture to evaluate models on iNaturalist 2018 dataset. We train the models for 100 epochs with the learning rate 0.1, decayed at 60 and 80 epochs by 0.1 with 10 linear warmup epochs. We also note that the value of weight decay (L2 regularization) matters a lot in the overall performance of this dataset, and we use a normed layer as a classifier following the literature. We finetune the classifier for 10 epochs with the learning rate annealed by cosine scheduling. The learning rate for fine-tuning is 3.0.

C Additional experimental results

This section provides additional results of our implementation for the main results and subgroup performance. Then we also present additional results for more analysis.

C.1 Main results

C.1.1 ImageNet-LT

We report three sub-groups performance (many, medium, and few) for ImageNet-LT dataset. Results are summarized in Table 7. While the performance of CP-Mix for Many sub-group is dropped by about 2% compared to balanced softmax, it significantly improves in Medium and Few sub-groups.

Method	Many	Medium	Few	All
Cross Entropy [†]	65.9	37.6	9.1	44.6
LDAM-DRW [†]	62.1	46.4	30.1	50.3
Balanced Softmax [†]	61.6	48.1	30.3	50.9
MiSLAS	61.7	51.3	35.8	52.7
CP-Mix [†]	59.3	53.5	39.7	53.9

Table 7: ImageNet-LT. [†] denotes results reproduced by us, and others are from the original papers.

C.1.2 Places-LT

Table 8 summarizes the results for Places-LT dataset. CP-Mix achieves significant improvement in overall performance compared to other baselines.

Method	Many	Medium	Few	All
Cross Entropy [†]	46.7	28.5	15.5	32.3
Balanced Softmax [†]	43.2	40.2	31.1	39.3
MiSLAS	39.6	43.3	36.1	40.4
CP-Mix [†]	45.4	42.7	36.1	42.3

Table 8: Places-LT. [†] denotes results reproduced by us, and others are from the original papers.

C.1.3 iNaturalist 2018

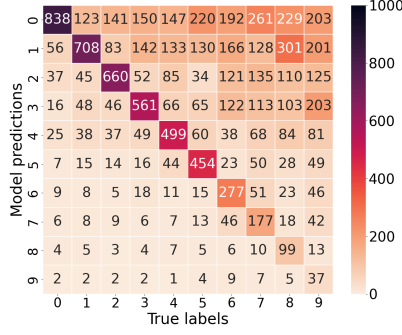
We report the result for iNaturalist 2018 dataset in Table 9. Although the performance drop of CP-Mix for Many sub-group seems significant, we note that the number of classes in Many sub-group is 842 among 8142 classes. Accordingly, CP-Mix achieves improvement for many classes at the cost of a decrease in a small number of classes. We note that weight decay affects the results significantly, with about 5% drop with 0.0005.

Method	Many	Medium	Few	All
Cross Entropy [†]	76.4	66.4	59.1	64.5
LDAM-DRW [†]	68.3	67.3	66.4	66.9
Balanced Softmax [†]	68.8	70.3	69.7	69.9
CP-Mix [†]	57.9	72.9	75.3	72.3

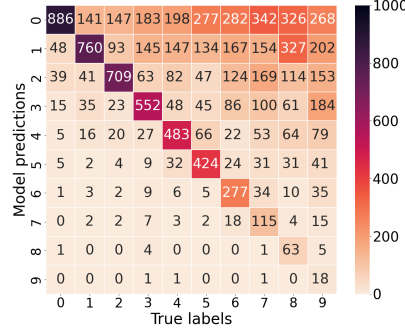
Table 9: iNaturalist 2018. [†] denotes results reproduced by us, and others are from the original papers.

C.2 Confusion matrix

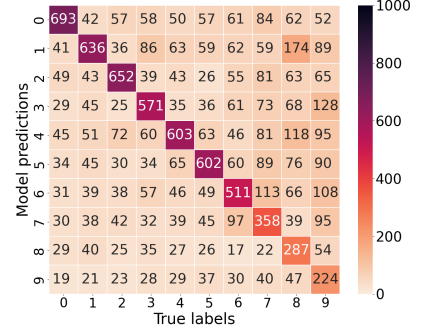
Figure 5 and Figure 6 demonstrate the confusion matrices of ERM, Mixup and CP-Mix classifiers trained on different CIFAR-LT datasets. CP-Mix successfully resolves the confusion-pairs and achieves significant performance improvement.



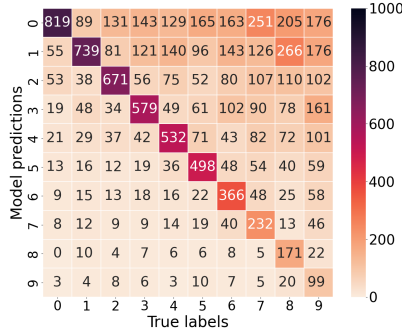
(a) ERM, CIFAR100-LT-100 dataset.



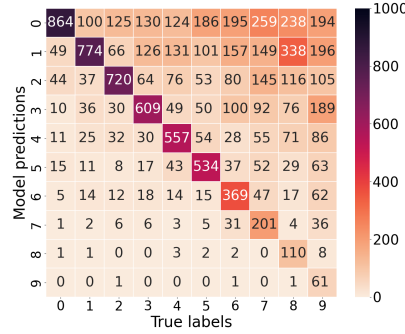
(b) Mixup, CIFAR100-LT-100 dataset.



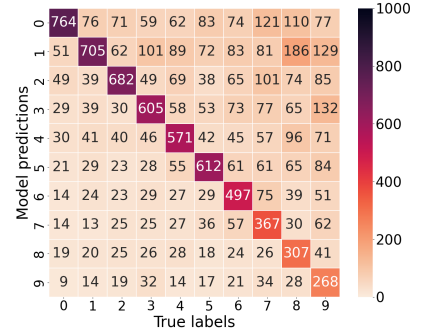
(c) CP-Mix, CIFAR100-LT-100 dataset.



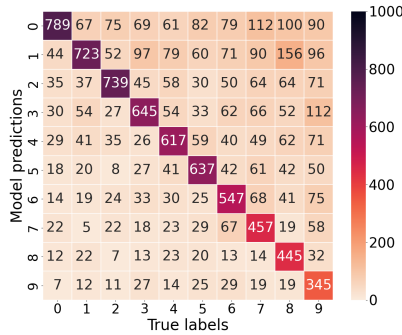
(d) ERM, CIFAR100-LT-50 dataset.



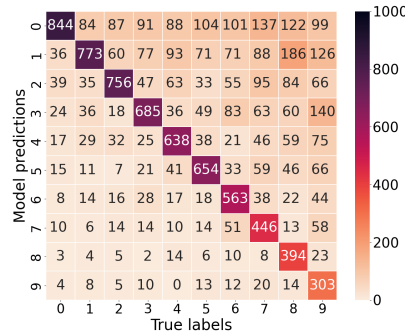
(e) Mixup, CIFAR100-LT-50 dataset.



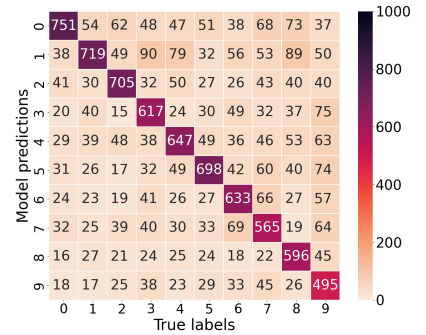
(f) CP-Mix, CIFAR100-LT-50 dataset.



(g) ERM, CIFAR100-LT-10 dataset.

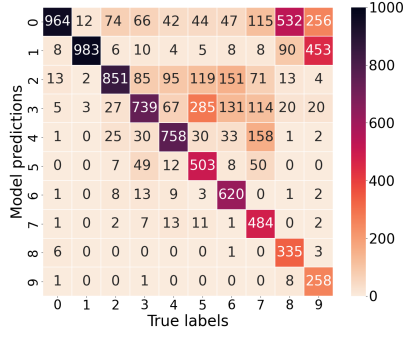


(h) Mixup, CIFAR100-LT-10 dataset.

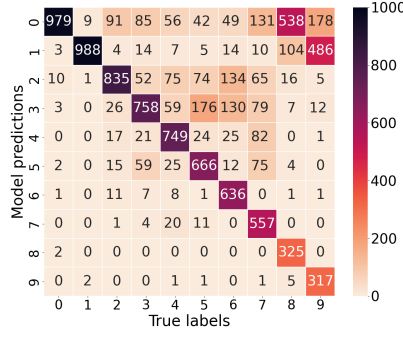


(i) CP-Mix, CIFAR100-LT-10 dataset.

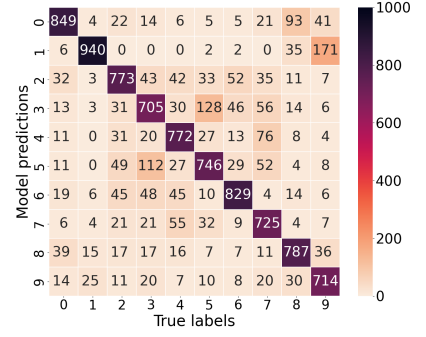
Figure 5: Confusion matrices of the ERM, Mixup and CP-Mix classifiers trained on CIFAR100-LT datasets.



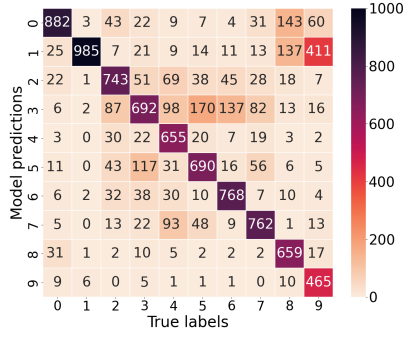
(a) ERM, cifar10-LT-200 dataset.



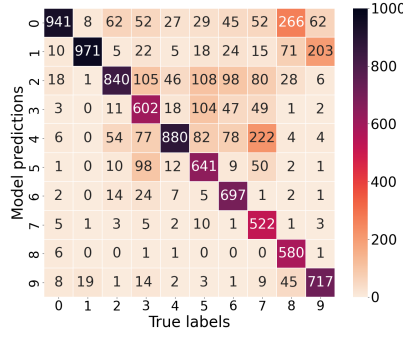
(b) Mixup, cifar10-LT-200 dataset.



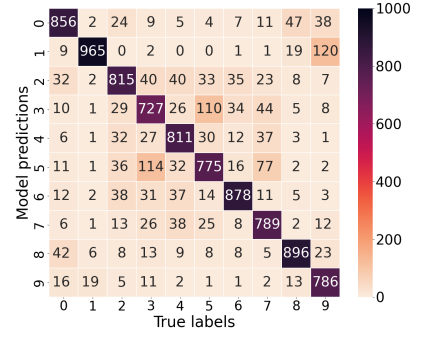
(c) CP-Mix, cifar10-LT-200 dataset.



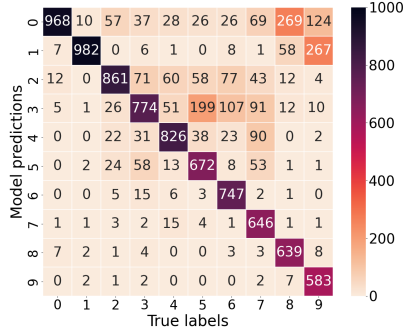
(d) ERM, cifar10-LT-100 dataset.



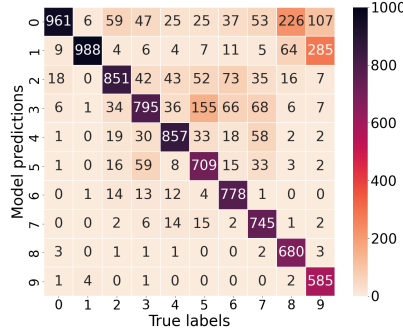
(e) Mixup, cifar10-LT-100 dataset.



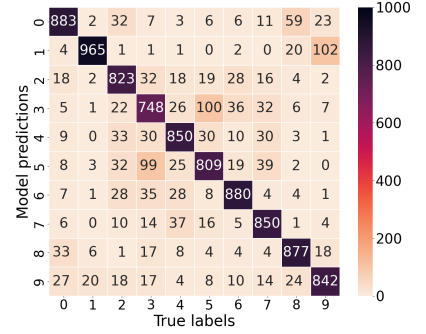
(f) CP-Mix, cifar10-LT-100 dataset.



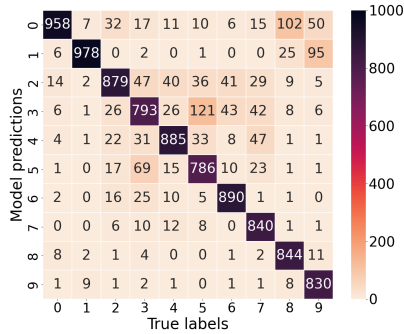
(g) ERM, cifar10-LT-50 dataset.



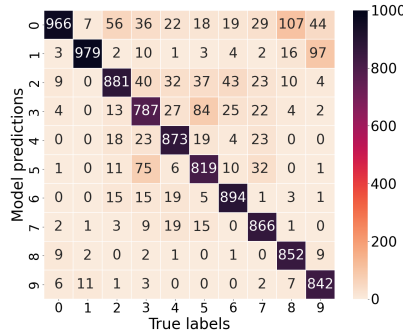
(h) Mixup, cifar10-LT-50 dataset.



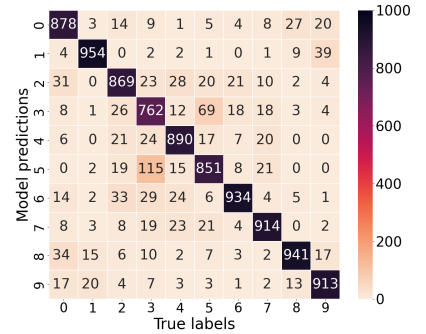
(i) CP-Mix, cifar10-LT-50 dataset.



(j) ERM, CIFAR10-LT-10 dataset.



(k) Mixup, CIFAR10-LT-10 dataset.



(l) CP-Mix, CIFAR10-LT-10 dataset.

Figure 6: Confusion matrices of the ERM, Mixup and CP-Mix classifiers trained on CIFAR10-LT datasets.